

## Article

# The Adhesion and Moisture Damage Resistance between Castor Oil-Based Bio-Asphalt and Aggregates under the Action of Thermal-Oxidative Aging

Ran Zhang <sup>1,2,3,\*</sup> , Qingwen Shi <sup>2</sup>, Pengkun Hu <sup>2</sup>, Jie Ji <sup>2,3</sup> and Long Wen <sup>4</sup>

<sup>1</sup> Key Laboratory of Road Structure and Material of Ministry of Transport (Changsha), Changsha University of Science & Technology, Changsha 410114, China

<sup>2</sup> School of Civil and Transportation Engineering, Beijing University of Civil Engineering and Architecture, Beijing 100044, China; shiqingwen1994@163.com (Q.S.); hupengkun2022@163.com (P.H.); jijie@bucea.edu.cn (J.J.)

<sup>3</sup> Beijing Urban Transportation Infrastructure Engineering Technology Research Center, Beijing 100044, China

<sup>4</sup> Department of Civil Engineering, Tsinghua University, Beijing 100084, China; longwen1102@163.com

\* Correspondence: zhangran@bucea.edu.cn; Tel.: +86-18302902812

**Abstract:** This study aims to investigate the adhesion properties and moisture damage resistance between castor oil-based bio-asphalt (COBA) and aggregates under the action of thermal oxidation. Different dosages of castor oil-based bio-oil (5%, 10%, and 15%) were used to prepare the COBA by mixing it with petroleum asphalt. The short-term and long-term aging of COBA were simulated by the rolling thin-film oven test (RTFOT) over 85 min and 385 min, respectively. The boiling method, photoelectric colorimetry, contact angle test, and contact angle moisture susceptibility test (CAMSIT) were used to evaluate the adhesion and exfoliation of the COBA–aggregates before and after thermal oxygen aging. Then, the aging degree of COBA was quantitatively evaluated by Fourier transform infrared (FTIR), and the correlation between aging condition and COBA–aggregates adhesion was analyzed. The results showed that the cohesion in COBA increased by 23.1% on average due to the addition of bio-oil. And the adhesion between COBA and aggregates increased by 5% due to the acidic compounds formed in the process of interaction with silicates on the surface of the aggregates. After short-term thermal oxidation, the adhesion between COBA and its aggregates was further improved as the polar components in the asphalt binder increased when the bio-oil dosage was less than 10%. However, with the continuous increase in the bio-oil amount and thermal oxidation degree, the adhesion decreased by 12.6% when compared to the virgin status; in addition, the adhesion grade decreased. Also, a low dosage of bio-oil was found to also improve COBA's resistance to moisture damage, and helped to reduce moisture sensitivity during the interaction with asphalt binder. However, the acidic compounds that were generated by the reaction with hydrolyzed aggregates in the presence of asphalt binder reduced the adhesion between COBA and the aggregates. Finally, FTIR revealed a good correlation between  $I_{C=O}$  and adhesion between COBA and the aggregates.

**Keywords:** castor oil-based bio-oil; bio-asphalt; thermal-oxidative aging; adhesion; moisture damage



**Citation:** Zhang, R.; Shi, Q.; Hu, P.; Ji, J.; Wen, L. The Adhesion and Moisture Damage Resistance between Castor Oil-Based Bio-Asphalt and Aggregates under the Action of Thermal-Oxidative Aging. *Appl. Sci.* **2023**, *13*, 10410. <https://doi.org/10.3390/app131810410>

Academic Editor: Syed Minhaj Saleem Kazmi

Received: 17 June 2023

Revised: 3 August 2023

Accepted: 31 August 2023

Published: 18 September 2023



**Copyright:** © 2023 by the authors. Licensee MDPI, Basel, Switzerland. This article is an open access article distributed under the terms and conditions of the Creative Commons Attribution (CC BY) license (<https://creativecommons.org/licenses/by/4.0/>).

## 1. Introduction

Bio-asphalt, as a new green environmental protection material, has a similar chemical composition to petroleum asphalt [1–3]. It can also save costs, reduce carbon emissions, and has good environmental benefits. Research has shown that the pyrolysis of biomass oil is not complete in the preparation process, and that it is susceptible to undergoing polymerization and esterification during storage, which increases its own viscosity [4,5]. Moreover, the polar and phenolic substances in bio-oil also can provide good adhesion performance by mixing it into petroleum asphalt. However, if the adhesion between asphalt

and the aggregates is reduced, then pavement loosening, potholes, and other distresses will occur. This affects road performance and service life under the long-term influence of the external environment (heat, light, oxygen, and water) [6,7].

Currently, various methods have been used to evaluate the adhesion of asphalt–aggregate interfaces. Júnior et al. [8] analyzed the influence of asphalt–aggregate adhesion on moisture resistance and the fatigue life of four different asphalt mixtures through digital image processing, a modified Lottman test, and the tensile compression test. As a result, it was found that the type of aggregate has a significant relationship with the moisture-induced damage resistance between asphalt and aggregates. Liu et al. [9] used photoelectric colorimetry to compare the adhesion of three asphalt binders, SK-90, SBS-MA, and HCRA-60, to limestone and basalt. Results showed that the asphalt binders still exhibited excellent adhesive properties after mixing a large amount of rubber powder and a small amount of waste oil into the base asphalt. Ji et al. [10] used surface free energy theory to study the contribution of direct coal liquefaction residue (DCLR) to asphalt–aggregate adhesion. It was demonstrated that, as the dosage of DCLR increased, the surface free energy and adhesion property of asphalt increased before and after aging, thus exhibiting good adhesivity. Huang et al. [11] evaluated the factors affecting the asphalt–aggregate bonding performance by improving the pull-off test. And it was found that the fractions of saturates, aromatics, resins, and asphaltenes (SARA) had the greatest influence on the bonding strength between asphalt and aggregates. Furthermore, asphaltene and resin can enhance the adhesion of the asphalt to the aggregate. Lyu et al. [12] evaluated the performance of bio-modified, rubberized asphalt under the conditions of thermal aging, UV aging, and moisture with the moisture-induced shear-thinning index (MISTI) and the contact angle moisture susceptibility test (CAMSI). They found that bio-oil could improve the resistance of asphalt to cohesion damage by three times, and that bio-oil could also retard the reaction of free radicals with asphalt.

Meanwhile, the aging and type of bio-asphalt also affects the adhesion performance of bio-asphalt–aggregate. Al-Sabaei et al. [13] found that the chemical composition of bio-asphalt made from different plant-originated bio-oil directly affects its sensitivity to aging. As a result, the adhesion of asphalt–aggregate under moisture damage conditions is significantly decreased. Zhao et al. [14] prepared bio-asphalt by adding timber-originated biochar to petroleum asphalt and tested its aging resistance. The results demonstrated that biochar could reduce the effect of aging on the performance of asphalt binders. Ingrassia et al. [15] found that the recycled asphalt binder containing bio-additives had a lower aging sensitivity, better mechanical properties, and less susceptibility to cracking than original asphalt. At the same time, Lv et al. [16] also observed that the high content of oxygen and light components in bio-oil also make bio-asphalt generally prone to aging. Therefore, the aging and moisture damage resistance of bio-asphalt is particularly important for the study of adhesivity in bio-asphalt–aggregate.

The current research on bio-asphalt is mainly focused on the influence of bio-oil on its performance. However, the adhesion performance and moisture damage resistance of bio-asphalt and aggregates when under the effect of aging have been less studied. In addition, bio-oil is widely available, and the difference of the preparation process can make the performance of bio-oil vary greatly. In this study, castor oil-based bio-asphalts (COBAs) were prepared by mixing 5%, 10%, and 15% of castor oil-based bio-oil with petroleum asphalt. The adhesion performance and moisture damage resistance of COBA–aggregate (limestone, slag) before and after thermal oxidation were evaluated by macroscopic tests such as the boiling test, photoelectric colorimetry, the contact angle test, and the CAMSI. Moreover, the adhesion mechanism and moisture damage resistance mechanism of the COBA–aggregate under thermal oxidation were revealed via the Fourier transform infrared (FTIR) test. This study provides theoretical support for the application of biomass resources in the field of road engineering, as well as promotes the sustainable development of transportation infrastructure.

## 2. Materials and Methods

### 2.1. Materials

#### 2.1.1. Base Asphalt

The base asphalt used is Sinopec 70# petroleum asphalt. Its relevant properties were tested according to the Standard Test Methods of Bitumen and Bituminous Mixtures for Road Engineering (JTG E20-2011) [17], and the results are shown in Table 1.

**Table 1.** Physical properties of base asphalt.

Property	Test Results	Specification	Technical Requirements	Reference Specification
Penetration (25 °C, 5 s, 100 g)/0.1 mm	63	T0604-2011	60~80	JTG F40-2004 [18]
Softening point/°C	44.5	T0606-2011	≥44	
Ductility (10 °C)/cm	45	T0605-2011	≥20	
Density/(g·cm <sup>−3</sup> )	1.043	T0603-2011	-	
Mass loss of RTFOT (163 °C, 85 min)/%	0.17	T0610-2011	≤±0.8	
Residual penetration ratio/%	63	T0604-2011	≥58	
Residual ductility (10 °C)/cm	8	T0605-2011	≥4	

#### 2.1.2. Bio-Oil

The bio-oil used is castor oil-based bio-oil. It is obtained by processing the residue left after the extraction of castor oil from castor seeds. And its basic properties are shown in Tables 2 and 3. The physical performance indicators of COBAs are shown in Table 4.

**Table 2.** Chemical components of bio-oil and base asphalt.

Types	Saturates/%	Aromatics/%	Resin/%	Asphaltene/%
Bio-oil	25.5	45.6	6.7	19.4
Base asphalt	26.6	51.8	6.8	14.8

**Table 3.** Physical and chemical characteristics of bio-oil and base asphalt.

Types	Elements (%)					Ash (%)	pH	Density (g/cm <sup>3</sup> )
	C	H	O	N	S			
Bio-oil	71.22	10.18	10.31	0.05	0.146	2.89	7.72	0.974
Base asphalt	84.31	10.23	0.79	0.85	3.75	—	7.52	1.043

**Table 4.** The physical performance indicators of COBAs.

Content (%)	Penetration (0.1 mm)	Softening Point (°C)	Ductility (10 °C/cm)	Acid Value (mgKOH/g)
0%	63	44.6	45	0.88
5%	84	41.9	122	0.94
10%	101	41.1	145	0.97
15%	124	40	150	0.99

#### 2.1.3. Aggregates

Limestone used commonly in road engineering and steel slag from industrial solid waste were selected as the aggregates. The surfaces of the aggregates had neither impurities nor obvious cracking, and their main chemical compositions are shown in Table 5.

**Table 5.** Chemical compositions of aggregates.

Aggregates	Main Oxide Content/%								
	CaO	MgO	SiO <sub>2</sub>	Fe <sub>2</sub> O <sub>3</sub>	Al <sub>2</sub> O <sub>3</sub>	SO <sub>3</sub>	P <sub>2</sub> O <sub>5</sub>	MnO	TiO <sub>2</sub>
Limestone	76.65	21.03	1.77	0.23	0.14	0.06	0.05	-	-
Steel slag	42.26	3.77	14.87	29.03	1.55	0.29	2.62	3.40	1.10

## 2.2. Test Methods

### 2.2.1. Preparation of Bio-Asphalts

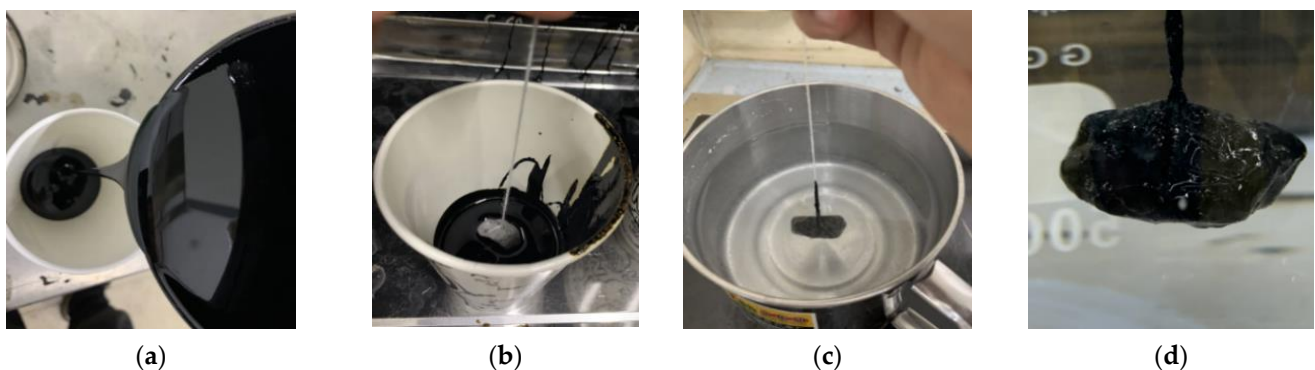
According to the previous research in our group [19], bio-oil has good compatibility with petroleum asphalt. Therefore, the shearing apparatus can be used to mix the bio-oil with the base asphalt under certain conditions. Firstly, the 70# asphalt binder was heated to 145 °C, as well as the heated bio-oil at 135 °C. Then, the bio-oil with amount of 5%, 10%, and 15% by weight were mixed with petroleum asphalt, respectively. Specifically, the mixing was performed at a rate of 3500 rpm at 130 °C for 15 min.

### 2.2.2. Aging Simulation of COBA

In this study, the rotating thin-film oven test (RTFOT) was used to simulate the short-term and long-term aging of COBA according to the T0610-2011 in JTG E20-2011 [17]. According to previous research [20,21], the heating time for short-term aging is 85 min, while long-term aging is 385 min as an equivalent replacement for PAV for 20 h.

### 2.2.3. Boiling Test

According to the relevant provisions of T0616-1993 in JTG E20-2011 [17], the boiling test is used to evaluate the resistance to moisture damage between COBA and aggregates. The adhesion of 4 kinds of COBAs and 2 kinds of aggregates (limestone, steel slag) before and after thermal oxidation was clarified. After the test, the peeling of asphalt film from the surface of the aggregate was observed and the adhesion grade was evaluated. The test process is shown in Figure 1, and each group of test was carried out with five parallel samples.

**Figure 1.** Process of boiling method. (a) Baking. (b) Soaking. (c) Boiling. (d) Observation.

### 2.2.4. Photoelectric Colorimetry

Since the asphalt film is easy to peel off from the surface of aggregates when soaked in water, phenol saffron is selected as the dye in this test. The absorbance of the residual dye solution after soaking the asphalt mixture is measured via ultraviolet spectrophotometer, after which its concentration is converted under the standard curve. As a result, the peeling degree of asphalt film is calculated using Equations (1)–(3).

Adsorption capacity of pure aggregate  $q$ :

$$q = \frac{(C_0 - C_1)V}{m} \quad (1)$$



Adsorption capacity of asphalt mixture after peeling test  $q'$ :

$$q' = \frac{(C_0 - C'_1)V}{m'} \quad (2)$$

where  $q$  and  $q'$  are the adsorption of phenol saffron by aggregate and asphalt mixture (mg/g), respectively;  $C_0$  is the starting solution concentration of phenol saffron solution (mg/mL);  $C_1$  and  $C'_1$  are the residual solution concentrations of phenol saffron solution after adsorption by aggregate and asphalt mixture (mg/mL), respectively;  $V$  is the volume of phenol saffron solution (mL); and  $m$  and  $m'$  are the weights of aggregate and asphalt mixture (g), respectively.

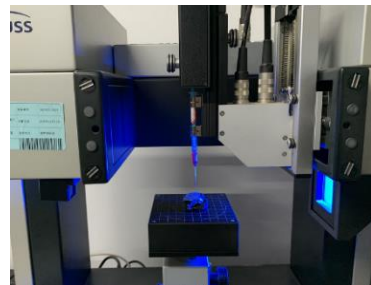
Stripping degree of asphalt from the surface of aggregate,  $St(q)$ :

$$St(q) = \frac{q'}{q} \times 100\% \quad (3)$$

The phenol saffron staining solutions are prepared at 0 mg/mL, 0.002 mg/mL, 0.004 mg/mL, 0.006 mg/mL, 0.008 mg/mL, and 0.01 mg/mL, respectively. The absorbance of the solutions with different phenol saffron concentrations is measured at a 510 nm wavelength. The relationship between the absorbance  $A$  and the concentration  $C$  of the solutions is  $A = 99.70871 \times C - 0.0003119$ ,  $R^2$  is 0.9998.

#### 2.2.5. Contact Angle Test

The contact angles of base asphalt, COBA, and aggregates were measured at 25 °C before and after thermal oxidation by using the sessile drop method. Four parallel tests were performed for each COBA sample and the same test liquid is measured three times on the same sample. The test schematic diagram is shown in Figure 2.



**Figure 2.** Contact angle test.

The test liquids are selected from distilled water, formamide, and ethylene glycol, which are stable at room temperature, have a large difference in surface free energy, and do not react with asphalt. The surface free energy parameters of the 3 test liquids at 25 °C are shown in Table 6, and the measured surface free energy of the aggregates and COBA are shown in Tables 7 and 8.

**Table 6.** Surface free energy parameters of test liquids at 25 °C.

Test Liquids	Surface Free Energy Parameters (mJ/m <sup>2</sup> )				
	$\gamma_L$	$\gamma_L^{LW}$	$\gamma_L^{AB}$	$\gamma_L^+$	$\gamma_L^-$
Distilled water	72.80	21.80	51.00	25.50	25.50
Formamide	58.00	39.00	19.00	1.92	39.60
Ethylene glycol	48.00	29.00	19.00	1.92	47.00

Note:  $\gamma_L$  is the total surface free energy of test liquid;  $\gamma_L^{LW}$  is the dispersion component of test liquid;  $\gamma_L^{AB}$  is the polarity component of test liquid;  $\gamma_L^+$  is the Lewis acid component of test liquid;  $\gamma_L^-$  is the Lewis base component of test liquid.

**Table 7.** Surface free energy parameters of aggregates.

Aggregates	Surface Free Energy Parameters (mJ/m <sup>2</sup> )				
	$\gamma$	$\gamma_d$	$\gamma_p$	$\gamma^+$	$\gamma^-$
Limestone	43.20	12.55	30.65	8.42	25.32
Steel slag	46.48	15.05	31.43	5.29	27.95

Note:  $\gamma$  is the total surface free energy of aggregates;  $\gamma_d$  is the dispersion component of aggregates;  $\gamma_p$  is the polarity component of aggregates;  $\gamma^+$  is the Lewis acid component of aggregates;  $\gamma^-$  is the Lewis base component of aggregates.

**Table 8.** Surface free energy parameters of COBA.

Aging Condition	Content of Bio-Oil (%)	Contact Angle (°)			Surface Free Energy Parameters (mJ/m <sup>2</sup> )					
		Distilled Water	Formamide	Ethylene Glycol	$\gamma$	$\gamma_d$	$\gamma_p$	$\gamma^+$	$\gamma^-$	Wa
Virgin	0	106.20	91.33	83.64	20.38	18.82	1.56	0.01	1.61	40.76
	5	104.11	88.40	85.40	23.00	21.33	1.67	0.02	1.73	46.00
	10	103.35	87.52	86.07	25.50	23.46	2.04	0.09	1.86	51.00
	15	103.04	87.00	87.12	26.78	24.56	2.22	0.14	1.88	53.56
RTFOT85	0	101.43	85.10	78.89	21.88	19.63	2.25	0.09	1.91	43.76
	5	102.50	85.56	78.98	23.57	21.61	1.96	0.005	1.64	47.14
	10	103.59	85.81	82.82	26.05	24.49	1.56	0.05	1.35	52.10
	15	104.48	86.34	78.69	27.69	26.50	1.19	0.20	1.19	55.38
RTFOT385	0	100.90	83.79	76.13	18.19	16.23	1.96	0.68	1.68	36.38
	5	101.85	84.53	77.06	18.80	17.43	1.37	0.40	1.53	37.60
	10	102.02	84.94	78.56	19.92	18.65	1.27	0.20	1.60	39.84
	15	103.00	85.20	79.23	22.83	21.83	1.00	0.10	1.36	45.66

Note: Wa is the cohesive work of COBA.

The calculation formulas of the cohesion work (Wa), the adhesion work (Was), the exfoliation work (Wasw), and the compatibility ratio (CR) of COBA–aggregates were calculated by Young’s formula [22] using Equations (4)–(7):

Cohesion work:

$$w_a = 2\gamma_a \quad (4)$$

Work of adhesion:

$$W_{as} = 2\sqrt{\gamma_a^d \gamma_s^d} + 2\sqrt{\gamma_a^p \gamma_s^p} \quad (5)$$

Work of exfoliation

$$W_{asw} = 2\sqrt{\gamma_a^d \gamma_w^d} + 2\sqrt{\gamma_s^d \gamma_w^d} + 2\sqrt{\gamma_w^+}(\sqrt{\gamma_a^-} + \sqrt{\gamma_s^-}) + 2\sqrt{\gamma_w^-}(\sqrt{\gamma_a^+} + \sqrt{\gamma_s^+}) - 2\gamma_w^d - 2\sqrt{\gamma_a^d \gamma_s^d} - 2\sqrt{\gamma_a^+ \gamma_s^-} - 2\sqrt{\gamma_a^- \gamma_s^+} - 4\sqrt{\gamma_w^+ \gamma_w^-} \quad (6)$$

Compatibility ratio:

$$CR = \frac{|W_{as}|}{|W_{asw}|} \quad (7)$$

where  $\gamma_a$ ,  $\gamma_a^d$ , and  $\gamma_a^p$  are the total surface free energy, the dispersion component, and the polarity component of asphalt, respectively;  $\gamma_s^d$  and  $\gamma_s^p$  are the dispersion component and the polarity component of stone, respectively;  $\gamma_w^d$  and  $\gamma_w^p$  are the dispersion component and the polarity component of water, respectively;  $\gamma_a^+$  and  $\gamma_a^-$  are the Lewis acid component and Lewis base component of asphalt, respectively;  $\gamma_s^+$  and  $\gamma_s^-$  are the Lewis acid component and Lewis base component of stone, respectively; and  $\gamma_w^+$  and  $\gamma_w^-$  are the Lewis acid component and Lewis base component of water, respectively.

### 2.2.6. Contact Angle Moisture Susceptibly Test

In this test, the interaction between COBA and siliceous aggregates was evaluated using the interfacial energy between asphalt and glass slide [12]. Firstly, the surface of the glass slide was cleaned with distilled water and anhydrous ethanol to remove the impurities. Secondly, 15 mg COBA was poured on the glass slide and heated in the oven at 140 °C for 10 min to simulate the contact angle of COBA with the glass slide in the molten state. And then the COBA was cooled at room temperature to ensure that COBA could form a contact angle on the surface of the glass slide. For the samples of water conditioning, the previously obtained dry samples were placed in a water bath in distilled water at 80 °C for 2 h, and then cooled and dried on the surface at room temperature. Finally, the contact angle of base asphalt and COBA before and after water conditioning was measured at 25 °C. Moreover, the contact angle moisture susceptibility index (CAMSII) of COBA was calculated using Equation (8):

$$\text{CAMSII} = \frac{\text{Contact Angle}_{\text{wet}} - \text{Contact Angle}_{\text{dry}}}{\text{Contact Angle}_{\text{dry}}} \quad (8)$$

### 2.2.7. Fourier Transform Infrared Reflection (FTIR) Test

In this test, the Nicolet iS10 FTIR instrument was used to characterize the microstructure of bio-oil, base asphalt, and COBA using ATR mode. The wave number range is 4000–500  $\text{cm}^{-1}$  with 32 scans. The carbonyl group index ( $I_{\text{C=O}}$ ) and sulfoxide group index ( $I_{\text{S=O}}$ ) were calculated by Equations (9) and (10) to quantitatively analyze the aging degree of COBA:

$$I_{\text{C=O}} = \frac{A_{1705\text{cm}^{-1}}}{\sum A_{4000\text{cm}^{-1} \sim 600\text{cm}^{-1}}} \quad (9)$$

$$I_{\text{S=O}} = \frac{A_{1030\text{cm}^{-1}}}{\sum A_{4000\text{cm}^{-1} \sim 600\text{cm}^{-1}}} \quad (10)$$

where:  $\sum A = A_{2920} + A_{2852} + A_{1705} + A_{1600} + A_{1455} + A_{1375} + A_{1030} + A_{864} + A_{810} + A_{744} + A_{723}$ .


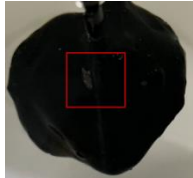

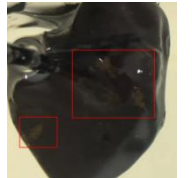


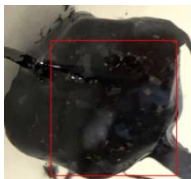


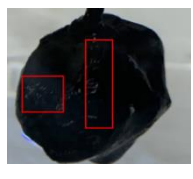








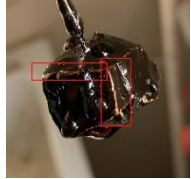

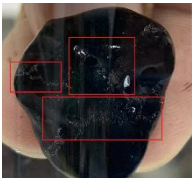



## 3. Results and Discussion

### 3.1. The Boiling Results

The results of the boiling test are shown in Table 9. The stripping section of the asphalt film has been marked with a red frame, and the corresponding adhesion grades are shown in Table 10.

It can be seen from Tables 9 and 10 that with the increase in bio-oil dosage, the overall peeling area of the asphalt film from the aggregates was slightly increased. The low content of bio-oil could improve the adhesion of COBA and aggregate, while the opposite was true for the high content of bio-oil. For instance, when the content of bio-oil was 5%, there was no obvious asphalt film shedding on the surface of the aggregates. When the content of bio-oil was 10%, the slag surface started to show patchy peeling and a small quantity of the asphalt film peeled off from the surface of the limestone, but this peeling area was still smaller than that of base asphalt. While the content of bio-oil was 15%, the peeling area of asphalt film on the surface of limestone was further increased. This is due to the fact that the added bio-oil increases the acid value of asphalt, and the acid molecules in asphalt will bind to the active site on the surface of the aggregate silicate to form alkyl acids, and then crystallize to form adhesions [23]. However, this acidic compound is easy to hydrolyze in water, which will weaken the moisture damage resistance of the COBA–aggregate. Therefore, during the boiling process, the more serious the hydrolysis process of the accumulated alkyl acids on the surface of the aggregates coated by COBA with high bio-oil dosage, the larger the area of asphalt-film peeling.

**Table 9.** Test results of the boiling method.

Content of Bio-Oil/%		0	5	10	15
Virgin	Limestone				
	Steel slag				
RTFOT85	Limestone				
	Steel slag				
RTFOT385	Limestone				
	Steel slag				

**Table 10.** Adhesion grade of COBA and aggregate.

Aging Condition	Aggregates	Content of Bio-Oil/%			
		0	5	10	15
Virgin	Limestone	4	4	4	4
	Steel slag	4	4	4	4
RTFOT85	Limestone	4	4	4	3
	Steel slag	4	4	4	3
RTFOT385	Limestone	3	3	3	3
	Steel slag	3	3	3	3

Note: Larger numbers represent the better adhesion levels of asphalt.

Under the action of short-term thermal oxidation, the adhesion between COBA and the aggregates was basically the same as the virgin status, only the adhesion grade of 15% COBA and the aggregates decreased to 3. However, the peeling degree of the asphalt film

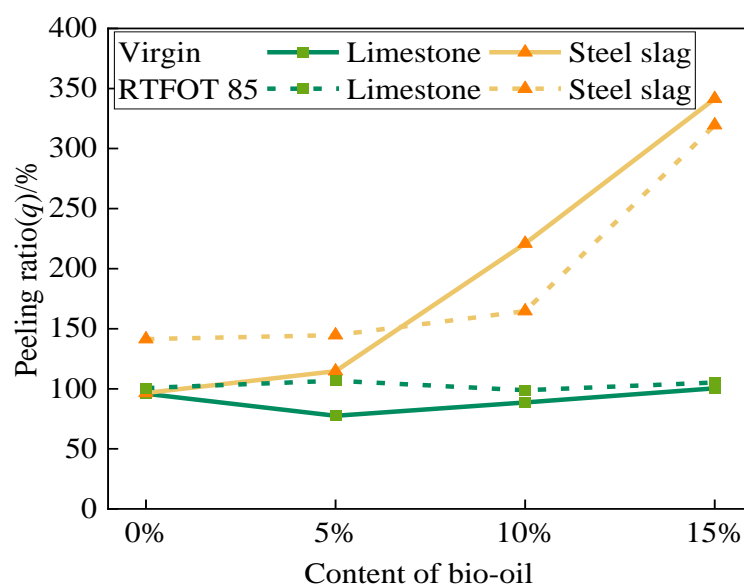
was aggravated after long-term aging, which led the peeling area to exceed 10%. This is due to the fact that COBA becomes hard and brittle under thermal oxidation, and 15% COBA with a higher bio-oil dosage is more prone to aging. Secondly, the polarity of water is much larger than COBA, and its diffusion ability on the surface of the aggregates is stronger. Therefore, the water can displace the asphalt film from the surface of aggregates more easily, thus reducing the adhesion grade of COBA–aggregate.

Under the same conditions, the adhesion grade of COBA and limestone was the same as that of steel slag, but the peeling positions of asphalt film were slightly different. The steel slag is more hygroscopic and has a rough surface, so the aged COBA is more likely to be peeled off from the surface of the steel slag. Meanwhile, the main mineral phase of limestone is alkaline  $\text{CaCO}_3$ , which can react with acidic compounds in COBA to produce some water-insoluble sticky substances. Therefore, the asphalt film on the surface of limestone is more likely to peel off at the corners and uneven edges.

Since the results of the boiling test are affected by several factors such as the angle of the aggregate, the surface roughness, and the thickness of the asphalt film, only a rough qualitative evaluation of the adhesivity of the COBA and aggregates can be made. To accurately distinguish the relationship of the moisture damage resistance of COBA and aggregates under the same adhesion grade, it needs to be further determined through other tests.

### 3.2. The Photoelectric Colorimetry Results

In this study, the peeling ratio of asphalt film from aggregates before and after thermal oxidation was calculated, and the results are shown in Figure 3.



**Figure 3.** Peeling ratio of COBA before and after thermal oxygen aging.

As shown in Figure 3, the peeling ratio of the COBA film from the steel slag exceeded 100% before and after thermal oxidation. Meanwhile, the same phenomenon was observed for COBA and limestone after thermal oxidation, which does not match the actual outcome. This phenomenon persisted after three parallel tests, which we considered to have been a result of a strong absorption impact by the test materials on the phenol saffron solution, thus interfering with the test results.

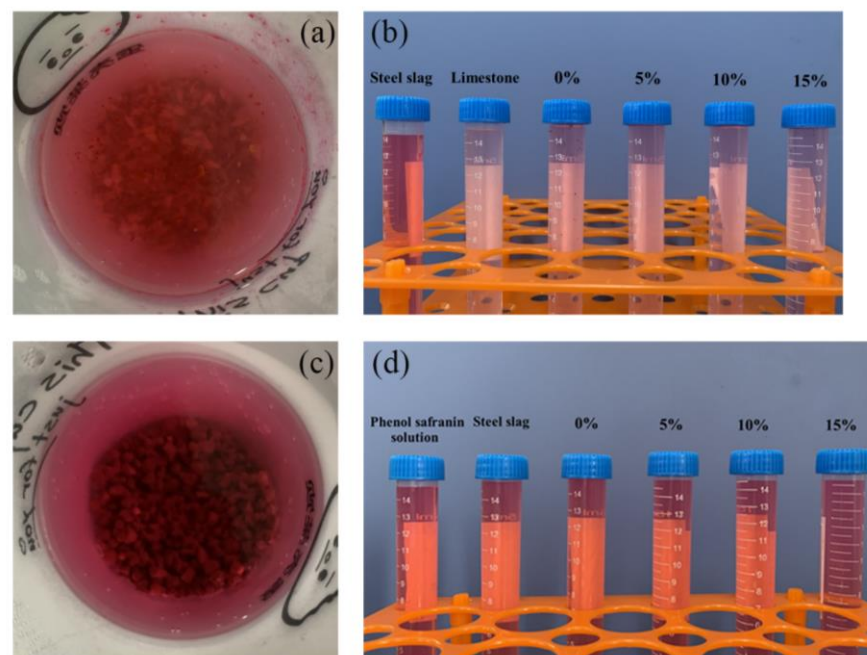
Since biomass heavy oil is an agricultural forestry waste and steel slag is an industrial solid waste, few have applied them in road engineering, and related studies have not yet been found. The feasibility of photoelectric colorimetry for evaluating the adhesivity of common asphalt and aggregates has been previously demonstrated. Therefore, for the



phenomenon of peeling ratio greater than 100%, this study is focused on analyzing the adsorption of phenol saffron solution by steel slag, limestone, and castor oil-based bio-oil.

From Figure 4, it can be seen that the adsorption ratio of limestone to phenol saffron after the water bath was 4–5 times higher than before. However, the adsorption ratio of steel slag to phenol saffron was only 6–7%, essentially indicating no adsorption. In addition, after the water bath, the residual concentration of phenol saffron in the solution containing steel slag mixture was lower than that only containing steel slag, demonstrating the adsorption to the phenol saffron of COBA. At the same time, the adsorption amount of COBA to phenol saffron was comparable to that of limestone when the COBA film was not exfoliated from the aggregate. This further confirmed the adsorption effect of COBA on phenol saffron. The peeling ratio was calculated by dividing the adsorption capacity of the asphalt mixture by the adsorption capacity of aggregates after the peeling test. As a result, the peeling ratio of the COBA film from the steel slag exceeded 100%, as shown in Figure 3.

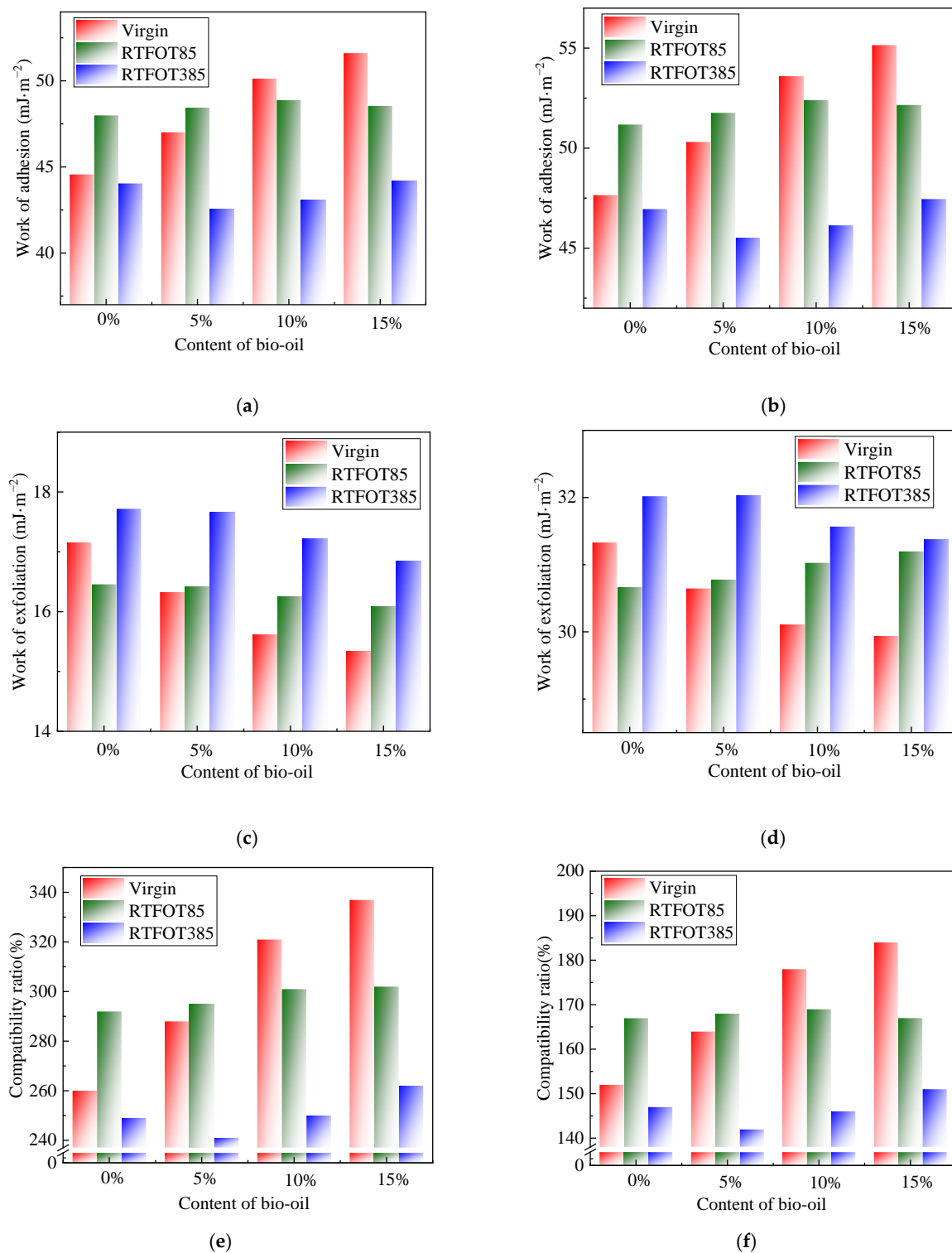
In summary, the adsorption of phenol saffron by COBA affects the peeling ratio of bitumen from the aggregate surface. Moreover, limestone and steel slag have a large difference in the absorption of phenol safranin. Therefore, the adhesion properties between COBA and different aggregates could not be evaluated directly using photoelectric colorimetry. However, the adhesion of the asphalt and aggregate of the same type can still be determined by observing the color difference between the residual solution and the standard solution, as shown in Figure 4b,d.



**Figure 4.** Adsorption of phenol saffron solution. (a) Limestone–phenol safranin solution. (b) Residual phenolic saffron solution after limestone–COBA absorption. (c) Steel slag–phenol safranin solution. (d) Residual phenolic saffron solution after steel slag–COBA absorption.

### 3.3. The Contact Angle Test Results

In this research, the contact angle, polar component, dispersion component, and surface free energy of the COBA and aggregates were measured using the sessile drop method. The results of cohesion work, the adhesion work, the exfoliation work, and the compatibility ratio of COBA–aggregate are shown in Figure 5.



**Figure 5.** COBA–aggregate adhesion under different aging states. (a) Work of adhesion (limestone–COBA). (b) Work of adhesion (steel slag–COBA). (c) Work of exfoliation (limestone–COBA). (d) Work of exfoliation (steel slag–COBA). (e) Compatibility ratio (limestone–COBA). (f) Compatibility ratio (steel slag–COBA).

#### (1) Surface free energy and cohesion work of COBA

As shown in Table 8, the surface energy and cohesion work of COBA increased with the increase in bio-oil addition and short-term thermal oxidation. For the virgin samples, the cohesion work of COBA increased by 12.9%, 25.1%, and 31.4%, respectively, compared

with the base asphalt when the bio-oil content was increased from 5% to 15%. After short-term aging, the surface energy and cohesion work of COBA increased by 4.0% and 16.4%, respectively, compared with the virgin sample. This indicated that the addition of bio-oil and short-term thermal oxidation could increase the cohesive properties of COBA.

## (2) Work of the adhesion of COBA–aggregate

The work of adhesion characterizes the adhesion performance between asphalt and aggregates under anhydrous conditions. The larger the work of adhesion value, the better the adhesion of asphalt to aggregates. According to Figure 5a,b, for the virgin samples, the work of adhesion between COBA and aggregates had an average increase rate of 5% with the increase in bio-oil content, among which, the adhesion work increased up to 15.7% when the bio-oil content was 15% compared with the base asphalt. This indicated that the bio-oil had a positive effect on the adhesion work between COBA and aggregates. After short-term aging, the effect of bio-oil content on the adhesion of COBA to aggregates was reduced. In addition, the work of the adhesion of base asphalt and 5% COBA to aggregates increased compared with virgin samples. This was because, after short-term aging, the light components in COBA gradually volatilized, and the macromolecular substances began to migrate qualitatively, which increased the polar components. The polar components adhered to aggregates via chemical adsorption, with high strength, which was not easy to be peeled off, so the adhesion was improved. However, the high content of bio-oil made COBA more prone to aging, and more resin were converted into asphaltene under thermal oxidation. Therefore, when the bio-oil content exceeds 10%, the adhesion between COBA and aggregate decreases. This is consistent with the decrease in adhesion grade via the boiling method.

After long-term aging, the adhesion work between COBA and aggregates was lower than that of base asphalt, and decreased by 12.6% on average compared to the virgin samples. This is due to the rapid increase in heavy components such as asphaltene and polar functional groups in COBA caused by long-term thermal oxygen, which makes the asphalt molecules harden. In addition, these components are easily converted into carboxylic acid and other substances under these conditions, making the asphalt brittle, thus leading to a decrease in the adhesion between COBA and aggregates.

In terms of the effect of aggregate type, the adhesion work between different aggregates and COBA increased at a similar rate with the increase in bio-oil content. However, the adhesion work between COBA and steel slag was higher. Before and after short-term thermal oxidation, the adhesion work between COBA and steel slag was 7% and 9% higher than that between COBA and limestone, respectively. The adhesion work between 15% COBA and steel slag was up to  $55.16 \text{ mJ/m}^2$ , which was 6.9% higher than that between COBA and limestone at the same bio-oil dosage. This was because the content of  $\text{SiO}_2$  in steel slag is higher than that in limestone, and the acid molecules in COBA are more likely to react with a high-valence metal salt to form alkyl acids, which accumulate and crystallize on the surface of aggregates to form adhesion [24]. Moreover, based on the physical adsorption theory, the greater the roughness of the aggregate surface, the more effective the contact area, and subsequently the more favorable to asphalt adsorption. Steel slag is also more conducive to COBA adsorption, forming adhesion because of its porous surface and higher roughness than limestone.

## (3) Work of exfoliation of COBA–aggregate

The work of exfoliation refers to the energy released by asphalt during the displacement of water from the surface of aggregates. The smaller the absolute value of exfoliation work, the greater the bonding strength of asphalt and aggregates under water conditions, and the stronger the ability of the mixture to resist water damage. According to Figure 5c,d, for the virgin samples, the exfoliation work between COBA and aggregates decreases with the increase in bio-oil content. This indicates that bio-oil exhibits the effect of improving the anti-stripping at the interface of asphalt–aggregate. Under the action of thermal oxidation, the work of the exfoliation of COBA increased, probably due to the decrease in internal

resin content and increase in asphaltene content in COBA after aging. This accordingly reduces the adhesion of COBA–aggregate, thus weakening its resistance to water damage.

In terms of aggregate type, the exfoliation work of COBA–limestone was much smaller than that of COBA–steel slag, which was only half of it. According to Table 4, the  $\text{SiO}_2$  dosage in steel slag was 8.4 times that in limestone, so COBA interacted with steel slag to form more acidic compounds, which could provide better adhesion. However, carboxylic acid compounds can ionize readily underwater and increase the moisture susceptibility of asphalt concrete, which results in a rapid decrease in the interfacial adhesion [25]. Also, the silicate in the aggregates and the H in the water produce a coulomb interaction and combine in the form of hydrogen bonds, causing steel slag to demonstrate a stronger hygroscopicity than limestone. In addition, the steel slag itself will have a hydration reaction with water, which can replace water during the hydration process, so the exfoliation work increases and the resistance to water damage stripping decreases.

#### (4) Compatibility ratio of COBA

The compatibility ratio is used to characterize the compatibility of asphalt and aggregates. The greater the compatibility ratio, the better the adhesion stability of the asphalt mixture. From Figure 5e,f, the compatibility ratio of COBA and limestone was twice higher than that of COBA and steel slag. The steel slag had a higher hygroscopicity and limestone was less affected by water, with a much lower exfoliation work than that of steel slag. Furthermore, with  $\text{CaCO}_3$  the as main component, limestone is more alkaline than steel slag, so it has a stronger acid-base reaction with COBA and better adhesion stability. Of course, the large adhesion work between steel slag and COBA is accompanied by large exfoliation work. This indicated that its adhesion with asphalt cannot work stably in the presence of water, which needs to be further explored.

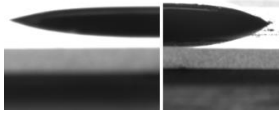
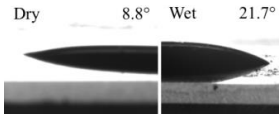
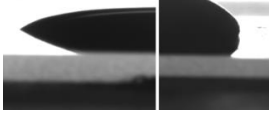
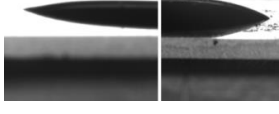
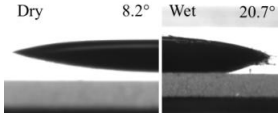
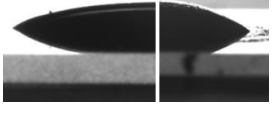
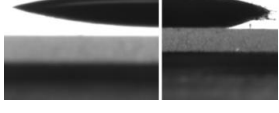
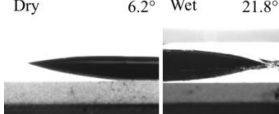
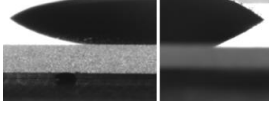
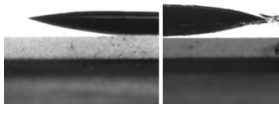
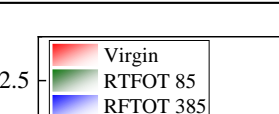
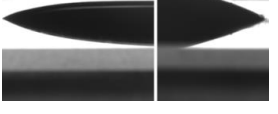
### 3.4. The Contact Angle Moisture Susceptibly Results

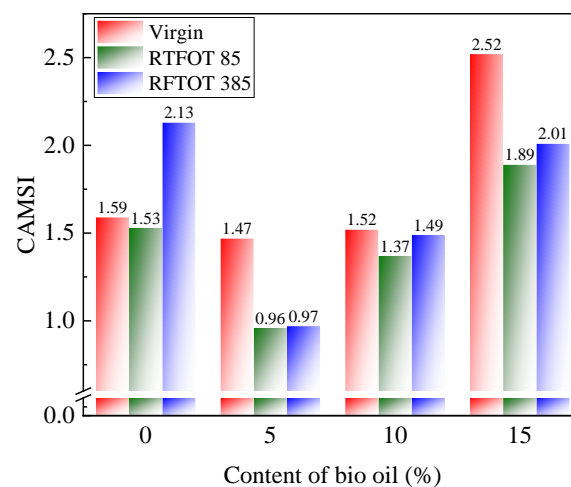
In this study, the moisture susceptibility of COBA was evaluated by observing the change in the contact angle of COBA before and after water conditioning on the slide surface. Typically, the smaller the contact angle, the better the adhesion of the asphalt to the solid surface [26]. The contact angle of COBA is shown in Table 11.

As observed in Table 11, for the virgin samples, the contact angle between COBA and the glass slide decreased with the addition of bio-oil before water conditioning. It demonstrated the increase in adhesion between asphalt and siliceous aggregates by bio-oil. With the process of water conditioning, the contact angle between COBA and the glass slide increased, indicating the decrease in adhesivity. This is because the affinity of COBA and water for  $\text{SiO}_2$  is different under chemically driven moisture damage [27]. Initially, COBA covers the surface of the dry slide with a low contact angle. But water gradually penetrates into the interface of COBA–slide and replaces COBA on the aggregates, increasing the contact angle between COBA and the glass slide.

After aging, the contact angle between COBA and the slide increased gradually. Under thermal oxidation, the light components in COBA decreased, accompanied by the increase in colloidal components, asphaltene, and other heavy components. As a result, the diffusion of COBA on the surface of the slide decreased and the contact angle increased. Meanwhile, the contact angle of COBA changed more after water conditioning, and the moisture damage resistance also changed significantly. Therefore, the moisture damage resistance of COBA was evaluated by calculating the CAMSI of COBA before and after thermal oxidation. The results are shown in Figure 6.

**Table 11.** Contact angle images of COBA before and after water conditioning.

Content of Bio-Oil/%	Aging Condition					
	Virgin		RTFOT 85		RTFOT 385	
0	Dry	9.1°	Wet	23.6°	Dry	18.1°
						
5	Dry	8.8°	Wet	21.7°	Dry	19.1°
						
10	Dry	8.2°	Wet	20.7°	Dry	15.4°
						
15	Dry	6.2°	Wet	21.8°	Dry	13.2°
						

**Figure 6.** CAMSI of COBA after thermo-oxidative aging.

The increase in CAMSI indicates a decrease in the adhesivity of asphalt with silica when it is exposed to water [12]. As shown in Figure 6, for the virgin samples, the CAMSI of mixtures with 5% and 10% COBA decreased by 7.5% and 4.4%, respectively, compared to base asphalt, while the CAMSI of mixtures with 15% COBA increased by 58.5%. This is consistent with the water-boiling method, demonstrating that low bio-oil dosage can improve the moisture damage resistance of COBA. This is due to the fact that low bio-oil dosage can better interact with asphalt and prevent moisture sub-penetration into the binder, reducing its moisture susceptibility [28]. In fact, while bio-oil changes the rheological properties of asphalt, it also weakens the durability of its mixture. The presence of a large amount of bio-oil in 15% COBA will cause the acidic compounds inside to diffuse rapidly and interact with the siliceous aggregate to produce carboxylic acid, etc. They will accumulate and crystallize at the interface of the aggregates, and then hydrolyze upon



contact with water, which is also the reason for the weakening adhesivity between the aggregates and COBA with a high dose of bio-oil [29,30].

Under the effect of thermal oxidation, the CAMSI after short-term aging was the smallest, while the CAMSI after long-term aging was even smaller than the original status. It demonstrated that COBA still has good adhesion property to silica when exposed to water and the short-term thermal oxidation effect has good advantage to improve the moisture damage resistance of COBA. Hung et al. found that the improved moisture damage resistance of bio-asphalt can be attributed to the ability of bio-oil to delay the formation of acidic compounds [31].

Rajib et al. [32] proposed that aged asphalt molecules have a higher interaction energy with  $\text{SiO}_2$  and thus can form more hydrogen bonds between the interface of the binder and the surface of  $\text{SiO}_2$ . In addition, the increased colloids and asphaltenes in the asphalt after thermal oxidation also play an important role in increasing the adhesion between COBA and aggregates. In general, the light components of COBA will evaporate after thermal oxygen, and the adhesion will also be slightly reduced. Ābele A et al. [33] found that using elastomers (SBS, rubber, etc.) to modify the bio-asphalt makes the polymer or rubber absorb the bio-oil to expand, thus improving the high- and low-temperature performance of the bio-asphalt. Therefore, the follow-up research group is also conducting research on the adhesion properties between composite modified bio-asphalt and aggregates.

### 3.5. FTIR Results

In this study, FTIR was used to compare and analyze the functional groups of COBA, as shown in Figure 7.

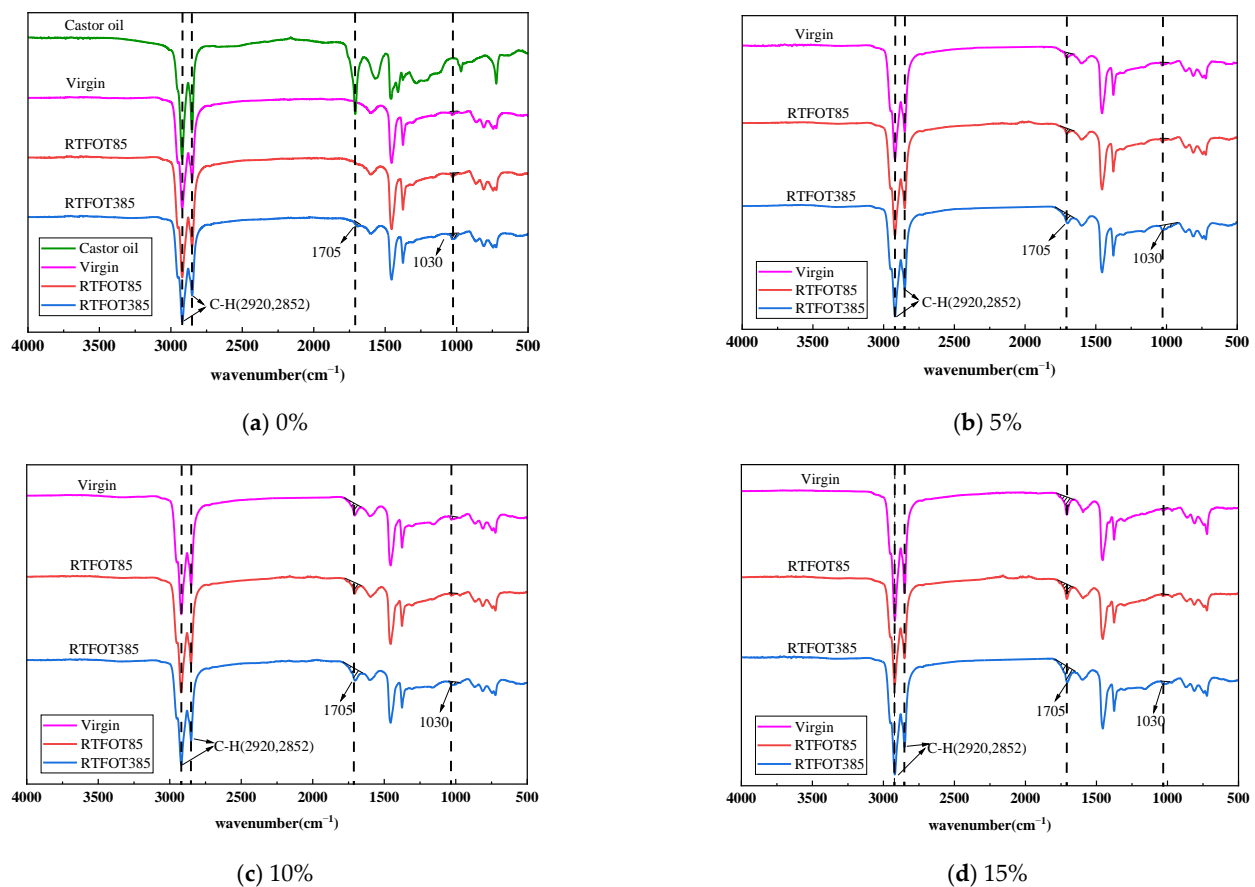


Figure 7. FTIR of castor oil-based bio-oil and COBA.

As shown in Figure 7, no new absorption peaks appeared in asphalt after the addition of bio-oil, but only the intensity of the peaks was different. Therefore, bio-oil was mainly physically dispersed in asphalt. As the thermal oxidation occurred, the area of characteristic peak for COBA at  $1705\text{ cm}^{-1}$  and  $1030\text{ cm}^{-1}$  increased gradually. It was found that asphalt is susceptible to thermal oxidation, resulting in the breaking of  $\text{C}=\text{C}$  to form  $\text{C}=\text{O}$ . At the same time, the H atoms are oxidized to hydroxyl groups, and the sulfur-containing functional groups react with oxygen to form the polar functional group of  $\text{S}=\text{O}$ . These increase the number of oxygen-sensitive functional groups inside asphalt. For example, the bio-oil showed a clear absorption peak of  $\text{C}=\text{O}$  at  $1705\text{ cm}^{-1}$ , and the larger the content of bio-oil, the more obvious the absorption peaks. Therefore, in order to quantify the variation of the oxygen-sensitive groups of COBA,  $I_{\text{C}=\text{O}}$  and  $I_{\text{S}=\text{O}}$  were calculated as shown in Figure 8.

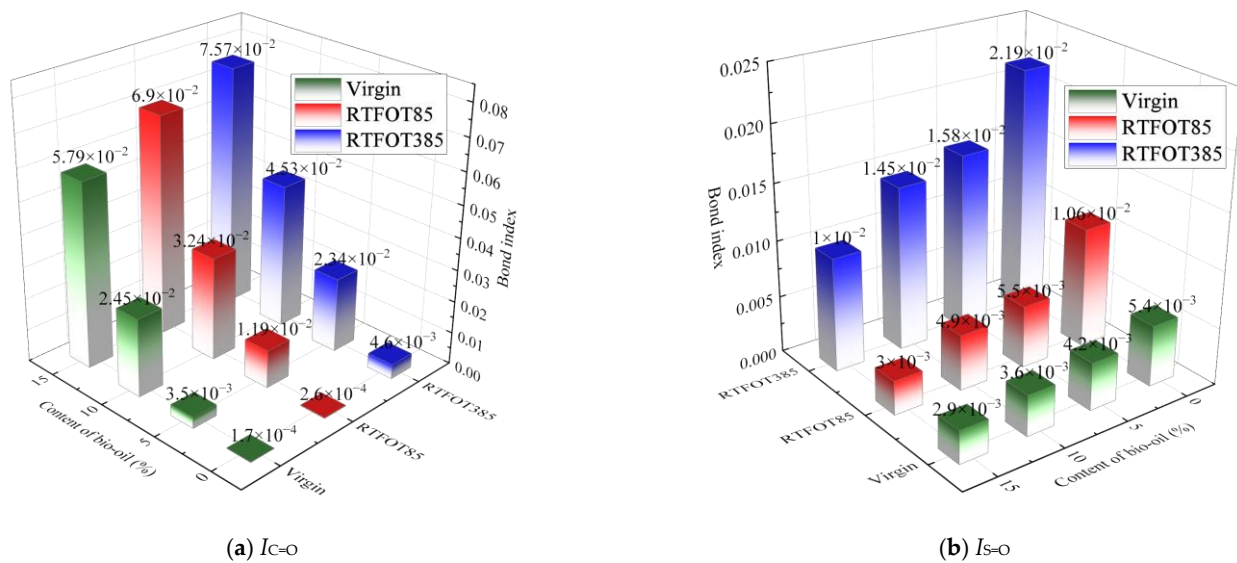


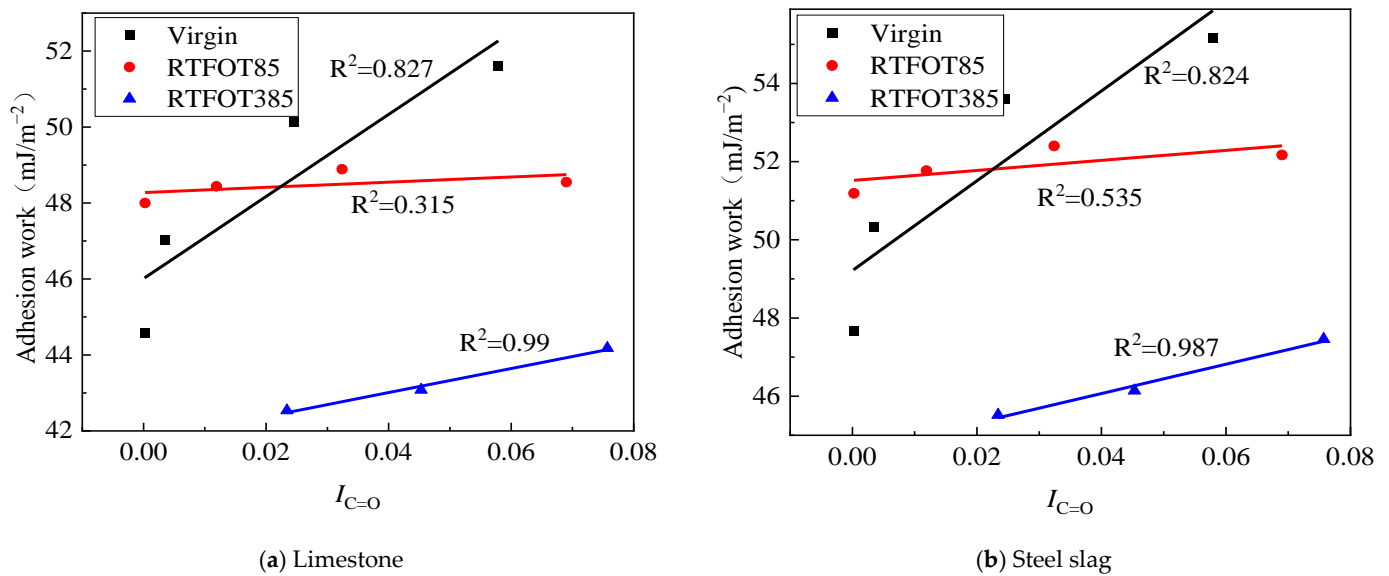
Figure 8. Functional group index of COBA.

According to Figure 8, the  $I_{\text{C}=\text{O}}$  increased 20, 144, and 340 times compared to that of base asphalt when the bio-oil content was increased from 5% to 15% in the virgin sample. However, the  $I_{\text{C}=\text{O}}$  of base asphalt was only  $1.7 \times 10^{-4}$ , which was extremely low, indicating that bio-oil brought a large amount of  $\text{C}=\text{O}$  to COBA. On the contrary,  $I_{\text{S}=\text{O}}$  decreased with increasing bio-oil, which is due to the very low content of S in bio-oil and the dilution of S content after blending with base asphalt.

Under thermal oxidation, the growth of  $I_{\text{C}=\text{O}}$  in COBA was similar in both short-term aging and long-term aging, while  $I_{\text{S}=\text{O}}$  grew rapidly in long-term aging. When the content of bio-oil increased from 5% to 15%,  $I_{\text{C}=\text{O}}$  increased by 2.4, 0.32, and 0.19 times compared to the virgin sample, respectively, after short-term aging; and 5.69, 0.85, and 0.31 times, respectively, after long-term aging.  $I_{\text{S}=\text{O}}$  increased by 0.03~0.36 and 2.45~3 times, respectively, in short-term and long-term aging, indicating that the production of  $\text{S}=\text{O}$  in COBA occurs mainly in the long-term aging. By considering the change of various groups in COBA and base asphalt before and after thermal oxidation, it can be assumed that the generation of  $\text{C}=\text{O}$  in COBA is mainly contributed by bio-oil, while  $\text{S}=\text{O}$  mainly originates from the base asphalt.

### 3.6. Correlation Analysis

As the  $I_{\text{C}=\text{O}}$  exhibited to have been the most sensitive to oxygen, the relationship of  $I_{\text{C}=\text{O}}$  to the adhesion of COBA-aggregate was analyzed before and after thermal oxygen aging, as shown in Figure 9.



**Figure 9.** Correlation between  $I_{C=O}$  and adhesion work and pull-out strength.

As illustrated in Figure 9, there is a high linear relationship between  $I_{C=O}$  of COBA and adhesion work between COBA and aggregates, and  $R^2$  is mostly around 0.9. This indicates that the change of COBA oxygen-sensitive functional groups before and after thermal oxidation is well correlated with the adhesion property of COBA–aggregate.  $I_{C=O}$  can be used as the evaluation index of asphalt–aggregate adhesion under thermal oxidation. After short-term aging, the  $R^2$  of  $I_{C=O}$  and adhesion work is low. This is likely because after short-term thermal oxidation,  $I_{C=O}$  increased with bio-oil content, and C=O with a higher concentration is easily converted to form alcohols and carboxylic acids, which makes the asphalt brittle. At the same time, C=O is prone to pyrolysis reaction at high temperatures, which makes the COBA molecular chain break, thus leading to asphalt aging and peeling. Notably, the increase in adhesion work between the COBA and aggregates is abrupt at 10% of bio-oil content, and the two follow an inconsistent trend change, so the correlation is low.

#### 4. Conclusions

In this study, the water-boiling method was used to observe the peeling area of asphalt film from the surface of aggregates and to obtain the adhesion grade. The surface free energy method was used to calculate the adhesion work and exfoliation work of COBA. Meanwhile, the moisture damage resistance of COBA was analyzed using the contact angle moisture susceptibility test. Finally, the quantitative evaluation of the aging of COBA was performed via FTIR, and the correlation between the aging of COBA and COBA–aggregate adhesion was analyzed. The following conclusions were drawn:

(1) Since COBA has a strong adsorption effect on phenosafranine, and steel slag has almost no absorption, photoelectric colorimetry is not suitable to evaluate the adhesion between steel slag and COBA.

(2) The cohesion in COBA increased by 23.1% on average due to the addition of bio-oil, and the adhesion between COBA and aggregates increased by 5% due to acidic compounds that formed in the process of the interaction with Si inside the aggregates.

(3) Under short-term aging, the work of adhesion between COBA and aggregates increased within a 10% dosage of bio-oil due to the increase in colloidal and polar substances in COBA. As the content of bio-oil and thermal oxidation degree continued to increase, the heavy component of COBA increased, and the excessive C=O content was converted to carboxylic acid and other substances that made asphalt brittle. At the same time, the microcracking of COBA during the aging process also increased the risk of moisture damage.

(4) Regarding the effect of aggregate types on COBA adhesion, the adhesion grades of COBA–limestone and COBA–steel slag were always consistent during the boiling process. Under dry conditions, steel slag formed acidic compounds and higher roughness; its work of adhesion with COBA was 7% and 9% higher than that of COBA–limestone before and after short-term thermal oxygen aging. However, under the influence of water, the acidic compounds that formed at the aggregate interface are easily hydrolyzed, and with the high hygroscopicity of steel slag and hydration reaction, the exfoliation work of COBA–slag is still higher than that of COBA–limestone.

(5) The change of oxygen-sensitive groups of COBA correlated well with the change of the adhesion of COBA–aggregate before and after thermal oxidation. And the adhesion performance of COBA–aggregate under thermal oxidation could be evaluated by calibrating the internal C=O content of COBA with the adhesion performance of COBA–aggregate.

**Author Contributions:** R.Z.: Methodology, writing—original draft, funding acquisition. Q.S.: Data curation, writing—original draft. P.H.: Data curation. J.J.: Conceptualization, methodology. L.W.: Conceptualization. All authors have read and agreed to the published version of the manuscript.

**Funding:** This study was financially supported by National Key R&D Program of China (2022YFB2601900), the National Natural Science Foundation of China (52208412), Research Project of Beijing Municipal Commission of Education (KM202210016009, KM202110016011), Open Fund of Key Laboratory of Road Structure and Material of Ministry of Transport (Changsha University of Science & Technology) (kfj210302), the Project of Construction and Support for High-Level Innovative Teams of Beijing Municipal Institutions (BPHR20220109).

**Institutional Review Board Statement:** Not applicable.

**Informed Consent Statement:** Not applicable.

**Data Availability Statement:** All data, models, and codes generated or used in this study are included in the submitted manuscript.

**Acknowledgments:** Thanks to Jiani Wang for her significant assistance in conducting the experiments.

**Conflicts of Interest:** The authors declare that they have no known competing financial interests or personal relationships that could have appeared to influence the work reported in this paper.

## References

1. He, L.; Tao, M.; Liu, Z.; Cao, Z.; Zhu, J.; Gao, J.; Van den bergh, W.; Chailleux, E.; Huang, Y.; Ma, Y.; et al. Biomass valorization toward sustainable asphalt pavements: Progress and prospects. *Waste Manag.* **2023**, *165*, 159–178. [\[CrossRef\]](#)
2. Chen, C.; Lu, J.; Ma, T.; Zhang, Y.; Gu, L.; Chen, X. Applications of vegetable oils and their derivatives as Bio-Additives for use in asphalt binders: A review. *Constr. Build. Mater.* **2023**, *383*, 131312. [\[CrossRef\]](#)
3. Ameri, A.; Haghshenas, H.F.; Fini, E.H. Future Directions for Applications of Bio-Oils in the Asphalt Industry: A Step to Sequester Carbon in Roadway Infrastructure. *Energy Fuels* **2023**, *37*, 4791–4815. [\[CrossRef\]](#)
4. Liu, Y.; Wang, D.; Ye, Y. Separation of Chemicals from Bio-oil and Their Application Prospects. *Chem. Ind. For. Prod.* **2013**, *33*, 137–143. (In Chinese)
5. Mohan, D.; Pittman, C.U., Jr.; Steele, P.H. Pyrolysis of wood/biomass for bio-oil: A critical review. *Energy Fuels* **2006**, *20*, 848–889. [\[CrossRef\]](#)
6. Yang, B.; Li, H.; Sun, Y.; Zhang, H.; Liu, J.; Yang, J.; Zhang, X. Chemo-rheological, mechanical, morphology evolution and environmental impact of aged asphalt binder coupling thermal oxidation, ultraviolet radiation and water. *J. Clean. Prod.* **2023**, *388*, 135866. [\[CrossRef\]](#)
7. Ding, Y.; Li, D.; Zhang, H.; Deng, M.; Mao, X.; Cao, X. Investigation of aging behavior of asphalt under multiple environmental conditions. *J. Mater. Civ. Eng.* **2022**, *34*, 04021419. [\[CrossRef\]](#)
8. Júnior, J.L.O.L.; Babadopulos, L.F.A.L.; Soares, J.B. Moisture-induced damage resistance, stiffness and fatigue life of asphalt mixtures with different aggregate-binder adhesion properties. *Constr. Build. Mater.* **2019**, *216*, 166–175. [\[CrossRef\]](#)
9. Liu, Q.; Liu, J.; Yu, B.; Zhang, J.; Pei, J. Evaluation and optimization of asphalt binder and mixture modified with high activated crumb rubber content. *Constr. Build. Mater.* **2022**, *314*, 125676. [\[CrossRef\]](#)
10. Ji, J.; Ma, R.; Zheng, W.; Suo, Z.; Xu, Y. Effect of Direct Coal Liquefaction Residue on Adhesion Characteristic between Asphalt and Aggregate. *China J. Highw. Transp.* **2018**, *31*, 27–33. (In Chinese)
11. Huang, G.; Zhang, J.; Wang, Z.; Guo, F.; Li, Y.; Wang, L.; He, Y.; Xu, Z.; Huang, X. Evaluation of asphalt-aggregate adhesive property and its correlation with the interaction behavior. *Constr. Build. Mater.* **2023**, *374*, 130909. [\[CrossRef\]](#)

12. Lyu, L.; Pei, J.; Hu, D.; Sun, G.; Fini, E.H. Bio-modified rubberized asphalt binder: A clean, sustainable approach to recycle rubber into construction. *J. Clean. Prod.* **2022**, *345*, 131151. [\[CrossRef\]](#)
13. Al-Sabaei, A.M.; Napiiah, M.B.; Sutanto, M.H.; Alaloul, W.S.; Usman, A. A systematic review of bio-asphalt for flexible pavement applications: Coherent taxonomy, motivations, challenges and future directions. *J. Clean. Prod.* **2020**, *249*, 119357. [\[CrossRef\]](#)
14. Zhao, S.; Huang, B.; Ye, X.P.; Shu, X.; Jia, X. Utilizing bio-char as a bio-modifier for asphalt cement: A sustainable application of bio-fuel by-product. *Fuel* **2014**, *133*, 52–62. [\[CrossRef\]](#)
15. Ingrassia, L.P.; Lu, X.; Ferrotti, G.; Conti, C.; Canestrari, F. Investigating the “circular propensity” of road bio-binders: Effectiveness in hot recycling of reclaimed asphalt and recyclability potential. *J. Clean. Prod.* **2020**, *255*, 120193. [\[CrossRef\]](#)
16. Lv, S.; Peng, X.; Liu, C.; Qu, F.; Zhu, X.; Tian, W.; Zheng, J. Aging resistance evaluation of asphalt modified by Buton-rock asphalt and bio-oil based on the rheological and microscopic characteristics. *J. Clean. Prod.* **2020**, *257*, 120589. [\[CrossRef\]](#)
17. *JTG E20-2011*; Standard Test Methods of Bitumen and Bituminous Mixtures for Highway Engineering. People’s Communications Press: Beijing, China, 2011.
18. *JTG F40-2004*; Technical Specifications for Construction of Highway Asphalt Pavements. China Communications Press: Beijing, China, 2004.
19. Zhang, R.; Wang, H.; Jiang, X.; You, Z.; Yang, X.; Ye, M. Thermal storage stability of bio-oil modified asphalt. *J. Mater. Civ. Eng.* **2018**, *30*, 04018054. [\[CrossRef\]](#)
20. Jiang, W.; Bao, R.; Lu, H.; Yuan, D.; Lu, R.; Sha, A.; Shan, J. Analysis of rheological properties and aging mechanism of bitumen after short-term and long-term aging. *Constr. Build. Mater.* **2021**, *273*, 121777. [\[CrossRef\]](#)
21. Tian, Y.; Li, H.; Zhang, H.; Yang, B.; Zuo, X.; Wang, H. Comparative investigation on three laboratory testing methods for short-term aging of asphalt binder. *Constr. Build. Mater.* **2021**, *266*, 121204. [\[CrossRef\]](#)
22. Yan, S.; Zhou, C.; Ouyang, J. Rejuvenation effect of waste cooking oil on the adhesion characteristics of aged asphalt to aggregates. *Constr. Build. Mater.* **2022**, *327*, 126907. [\[CrossRef\]](#)
23. Hung, A.M.; Pahlavan, F.; Shakiba, S.; Chang, S.L.; Louie, S.M.; Fini, E.H. Preventing assembly and crystallization of alkane acids at the silica-bitumen interface to enhance interfacial resistance to moisture damage. *Ind. Eng. Chem. Res.* **2019**, *58*, 21542–21552. [\[CrossRef\]](#)
24. Hung, A.M.; Mousavi, M.; Pahlavan, F.; Fini, E.H. Intermolecular interactions of isolated bio-oil compounds and their effect on bitumen interfaces. *ACS Sustain. Chem. Eng.* **2017**, *5*, 7920–7931. [\[CrossRef\]](#)
25. Fini, E.H.; Hung, A.M.; Roy, A. Active mineral fillers arrest migrations of alkane acids to the interface of bitumen and siliceous surfaces. *ACS Sustain. Chem. Eng.* **2019**, *7*, 10340–10348. [\[CrossRef\]](#)
26. Hosseinneshad, S.; Shakiba, S.; Mousavi, M.; Louie, S.M.; Karnati, S.R.; Fini, E.H. Multiscale evaluation of moisture susceptibility of biomodified bitumen. *ACS Appl. Bio. Mater.* **2019**, *2*, 5779–5789. [\[CrossRef\]](#)
27. Mousavi, M.; Oldham, D.; Fini, E.H. Using fundamental material properties to predict the moisture susceptibility of the asphalt binder: Polarizability and a moisture-induced shear-thinning index. *ACS Appl. Bio. Mater.* **2020**, *3*, 7399–7407. [\[CrossRef\]](#)
28. Nivitha, M.R.; Prasad, E.; Krishnan, J.M. Ageing in modified bitumen using FTIR spectroscopy. *Int. J. Pavement Eng.* **2016**, *17*, 565–577. [\[CrossRef\]](#)
29. Fan, Z.; Lin, J.; Chen, Z.; Liu, P.; Wang, D.; Oeser, M. Multiscale understanding of interfacial behavior between bitumen and aggregate: From the aggregate mineralogical genome aspect. *Constr. Build. Mater.* **2021**, *271*, 121607. [\[CrossRef\]](#)
30. Fini, E.H.; Samieadel, A.; Rajib, A. Moisture damage and its relation to surface adsorption/desorption of rejuvenators. *Ind. Eng. Chem. Res.* **2020**, *59*, 13414–13419. [\[CrossRef\]](#)
31. Hung, A.; Fini, E.H. Surface morphology and chemical mapping of UV-aged thin films of bitumen. *ACS Sustain. Chem. Eng.* **2020**, *8*, 11764–11771. [\[CrossRef\]](#)
32. Rajib, A.I.; Shariati, S.; Fini, E.H. The effect of progressive aging on the bond strength of bitumen to siliceous stones. *Appl. Surf. Sci.* **2021**, *550*, 149324. [\[CrossRef\]](#)
33. Ābele, A.; Merijs-Meri, R.; Bērziņa, R.; Zicāns, J.; Haritonovs, V.; Ivanova, T. Effect of bio-oil on rheological and calorimetric properties of RTFOT aged bituminous compositions. *Int. J. Pavement Res. Technol.* **2021**, *14*, 537–542. [\[CrossRef\]](#)

**Disclaimer/Publisher’s Note:** The statements, opinions and data contained in all publications are solely those of the individual author(s) and contributor(s) and not of MDPI and/or the editor(s). MDPI and/or the editor(s) disclaim responsibility for any injury to people or property resulting from any ideas, methods, instructions or products referred to in the content.